Astron. Astrophys. 345, 244–248 (1999)

ASTRONOMY AND ASTROPHYSICS

Properties of He-rich stars

II. CNO abundances and projected rotational velocities⋆

M. Zboril[1,2] **and P. North**[3]

[1] Armagh Observatory, Armagh, College Hill, BT61 9DG, Ireland
[2] Astronomical Institute, Tatranská Lomnica, 05960, Slovakia
[3] Institut d'Astronomie de l'Université de Lausanne, CH-1290 Chavannes-des-Bois, Switzerland

Received 26 January 1998 / Accepted 4 February 1999

Abstract. We present an abundance analysis of light elements in the most massive chemically peculiar (CP) stars, He-rich stars. The analysis is based on both low and high-resolution observations collected at ESO, La Silla, Chile in the optical region and includes 6 standard and 21 He-rich stars. Light element abundances display a diverse pattern from under-solar up to above-solar values. Carbon is found underabundant in the hottest He-rich stars and normal in the coolest ones, according to the LTE model predictions. The distribution of projected rotational velocities shows a significant excess of slow rotators, no He-rich stars having $v \sin i > 130$ km s^{-1}.

Key words: stars: abundances – stars: chemically peculiar

1. Introduction

The He-rich stars are the most massive CP stars. Their helium abundance ranges from nearly solar to larger than unity with respect to hydrogen. Spectroscopic and photometric variability is explained by an abundance distribution across the stellar surface. To explain the helium abundance itself a link between mass loss, abundance anomaly, radiative diffusion and magnetic field is suggested. Given standard atmospheric conditions in B-type stars (assuming no wind), diffusion is unable to support helium in the stellar atmosphere and helium sinks. However, Vauclair (1975) showed that diffusion could lead to He overabundance in the presence of stellar mass-loss. Models of abundance anomalies with selective mass-loss for He-rich stars suggest normal CNO abundances as a test (Michaud et al. 1987). More specifically, the model distinguishes between helium ionization degree, convective zone location, magnetic field configuration and stellar wind strength in the stellar atmosphere. Consequently, the CNO abundance pattern would depend on several parameters including effective temperature. In this contribution, we analyse both low and high-resolution ESO spectra to obtain light element abundances for He-rich stars and to put constraints on the theoretical model.

2. Observations

High-resolution spectra (resolving power 30000) were obtained using the CAT telescope and the CES spectrograph at ESO, La Silla, Chile, on 20–24 April 1992, in remote control mode from Garching. Helium and preliminary CNO abundances were described in Zboril, Glagolevskij & North (1994). The low resolution spectra (resolving power ∼4150) were obtained using the 1.5m spectrographic telescope and the Boller & Chivens spectrograph at ESO on 4–10 January 1993. Helium abundance analysis is described in Zboril et al. (1994) and Zboril et al. (1997). The total sample consists of 6 standard stars and 21 He-rich stars.

3. Abundance analysis

Given the instrumentation set-up, the abundance analysis from high-resolution spectra is based on the range 4235–4270 Å while low resolution spectra cover the 3952–4938 Å interval. Thus the optical region is fairly well covered; however, photospheric abundances are in general difficult to determine due to the weakness of the majority of photospheric lines. The UV resonance lines are much more pronounced but require exhaustive NLTE treatment. To start with, we derived carbon abundance and $v \sin i$ values from the 4268 Å line profile. The subsequent analysis is based on the best atmosphere models for early type stars, i.e. Kurucz (1992) models.

It turned out that it was better to put aside the constants for Stark broadening for the C II 4268 line and to apply instead the classical formula, $\Gamma_S \sim n_e.n_{eff}^5$, where n_e stands for electron plasma density and n_{eff} the effective quantum number of the upper level; otherwise, the line wings did not fit any of the observed line profiles. This effect was remarkably well established thanks to several cases where the $v \sin i$ value is equal to zero. Other damping constants (e.g. natural radiative) associated with broadening mechanisms matched the observations very well. Other line parameters, oscillator strengths etc.,

Send offprint requests to: M. Zboril

⋆ Based on observations collected at the European Southern Observatory, La Silla, Chile (programmes 7-043 and 7-010 of periods 49 and 50 resp.)

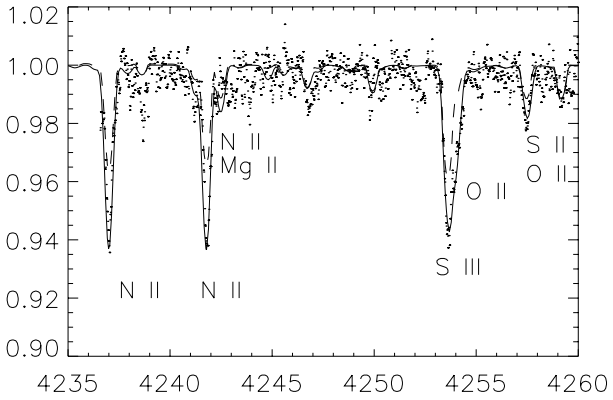

Fig. 1. A portion of the high-resolution spectrum of the reference star HD 122980 (*dots*) compared with synthetic spectra. *Solid* line: fits of N, O, Mg, S abundances, *dashed* line: solar abundances, $v \sin i = 20\ \mathrm{km\,s^{-1}}$. See text.

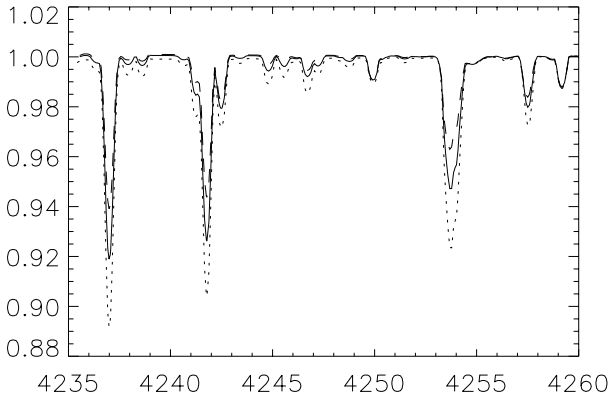

Fig. 2. A portion of synthetic spectrum vs. basic stellar parameters. *Solid* line: $\mathrm{T_{eff}} = 20000$ K, $\log g = 4.5$, *dashed* line: 20000 K, 4.0 and *dotted* line: 19000 K, 4.5.

have been maintained from the original Kurucz-Peytremann line list. Yet, tests have been made using other sources for atomic parameters, with values increased or decreased by 50 percent, but the pattern of CNO abundances did not change. The abundance analysis has been performed by a standard synthetic spectrum and LTE method. The number of well pronounced line profiles for light elements in the spectrum is not large enough to estimate reliably the microturbulent velocity and therefore we adopted a depth-independent microturbulent velocity value of $6\,\mathrm{km\,s^{-1}}$ (Kilian 1992). The abundance analysis is based on several lines reaching only a few percent of the continuum level (Fig. 1) which, unfortunately, were found to depend on basic stellar parameters, i.e. effective temperature and surface gravity (Fig. 2). This demonstrates already how fragile is the construction of CNO abundances vs. stellar age diagram. The analysis was primarily focused on prominent CNO photospheric lines while weaker as well as other lines (e.g. S, iron peak) will be analysed later except for the analysis of the prominent Mg II 4481 line profile.

4. CNO abundances

The abundances for light elements can be found in Table 1 and are displayed in Fig. 3. The column entitled "method" stands for the method of effective temperature and surface gravity determinations and the values are taken from Zboril et al. (1994) and Zboril et al. (1997). Fundamental parameters were derived by means of spectroscopy from hydrogen line profiles and using multi-colour photometry (Geneva, Strőmgren, UBV, whichever possible) in the case of high-resolution spectra where the hydrogen line profiles had not been observed. The spectral line profiles used in the abundance analysis were examined for atmospheric parameters sensitivity and turned out to be sensitive (Fig. 2). Therefore, we derived relevant partial derivatives by running a programme to obtain detailed line profiles for a number of model atmospheres. Subsequently, we used the standard formula of error propagation to derive the overall error bars. The gross effect on error bars was the following: 6–7% due to noise in the case of high-resolution data and three times that value for low-resolution data, as well as a decrease of the error on abundance with increasing effective temperature, especially for carbon. The values (1200 K, 0.2) as T_{eff} and $\log g$ error bars were accepted to express the possibilities of current techniques. Remarkably, errors on abundances from low-resolution data have reached considerable values for weak photospheric lines in stellar spectra.

The spread of light-element abundances (C, N, O) is similiar to the one found by previous authors (e.g. Osmer and Peterson 1974). These authors argued on significant scatter of light element abundances in He-rich stars. The spread in our sample in its purest form was checked by a working and temporary plot, namely $B - V$ vs. equivalent width. While the $B - V$ index may change typically up to 0.03 as some He-rich stars are variable, especially for high-resolution data the equivalent width increment for the same colour reaches 40%. However, the error bars on equivalent width are within 6–7%. Further complementary material also covering possible phase variations, as well as magnetic field measurements are necessary to reach more conclusive statements. Heavier elements such as magnesium appear to be insensitive to effective temperature and have a solar abundance except for extreme helium-rich stars where the magnesium spectral line is located in the wing of the helium one. The oxygen abundance has been determined using the λ4254 S III+O II blend in the high-resolution data (Fig. 1) and should be considered as a rough estimate only.

5. Projected rotational velocity distribution

In this section we show the projected rotational velocity distribution defined as the number of stars per interval ($vsini$ bin) divided by the total sample size and by the width of the interval. Similarly to the past studies, we adopted intercomparison with normal B-type stars. The distribution of normal stars was adopted from Wolff et al. (1982) who measured 306 early B-type stars based on intermediate reciprocal resolution, $\sim 15\,\mathrm{\AA mm^{-1}}$. Fig. 5 displays the comparison of He-rich stars and normal B-type stars distributions. A previous study of Wal-

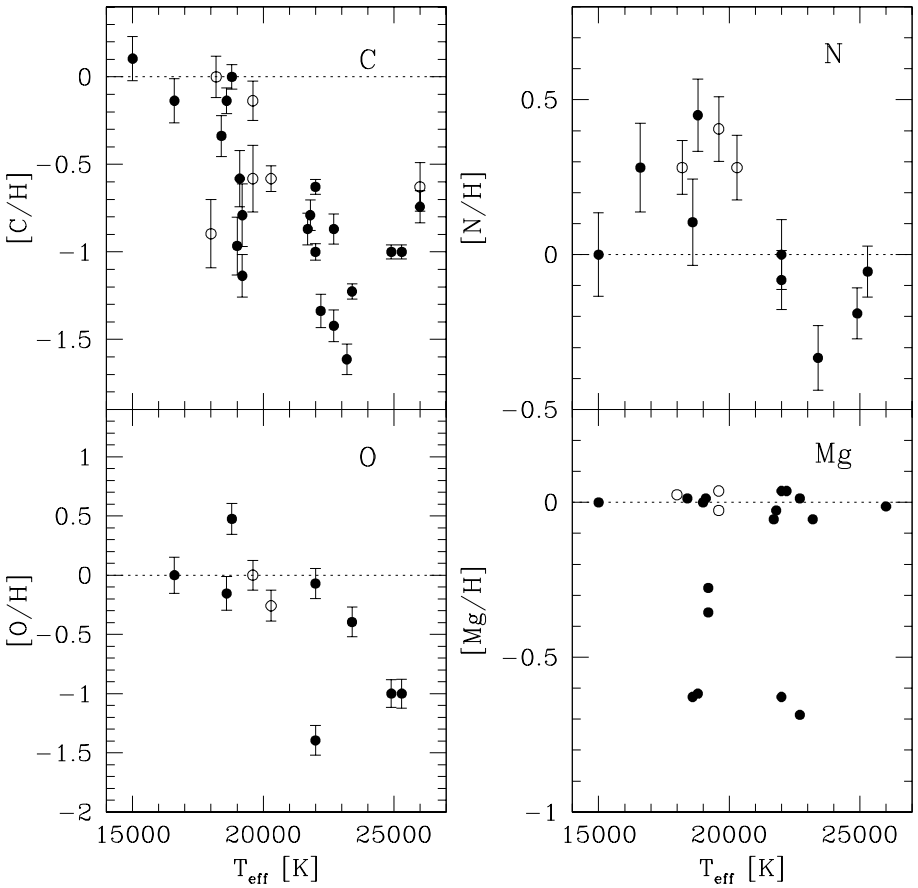

Fig. 3. Ratio of stellar to solar abundance (logarithmic scale) versus effective temperature. Key to symbols: *open circles* data for normal stars, *filled circles*: data for He-rich stars.

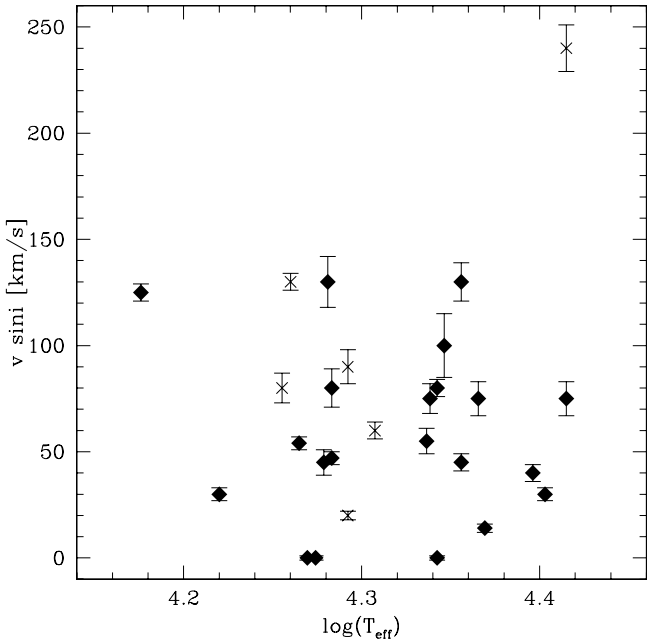

Fig. 4. $V\,sini$ value vs. logarithm of effective temperature. *diamonds:* He-rich stars, *crosses:* normal reference stars.

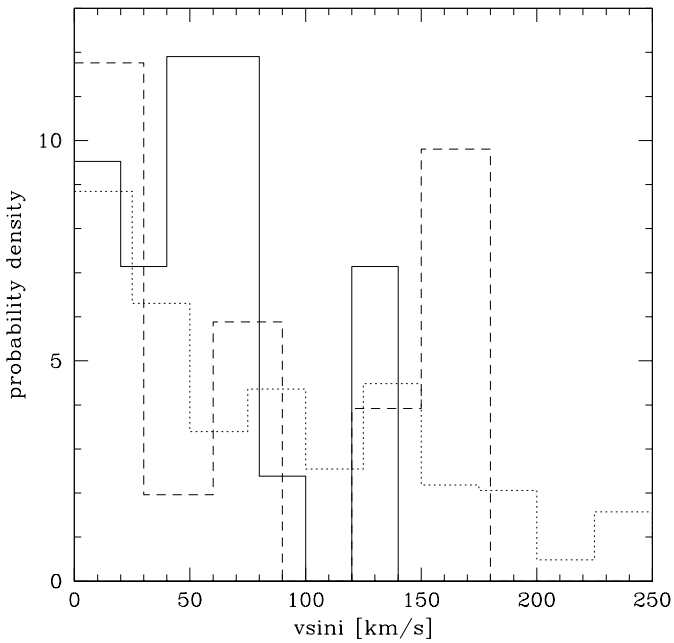

Fig. 5. Projected rotational velocity distribution (probability density) defined as the number of stars per interval divided by the total sample size and by the width of the interval and multiplied by 10^3. *Solid line:* He-rich stars, *dotted line:* normal B-type stars, Wolff et al. (1982), *dashed line:* He-rich stars after Walborn (1983).

Table 1. Elemental abundances in He-rich stars (upper part of the table) and in normal, reference stars (lower part). The reference normal stars, solar abundances, mean values from Kilian (1992) and ours are listed at the very bottom. The DM numbers obey the HD rule. In the second column, 4-digit numbers are HR ones and 5-digit numbers are HIP ones, unless a letter indicates otherwise; the letter S stands for SAO and N for NGC. Total error bars on abundances in percent. The $vsin\,i^*$ symbol stands for Walborn's data.

HD...	HR/HIP	$T_{\rm eff}$	method	$\log g$	C	N	O	Mg	$v \sin i$	$v \sin i^*$
36485	1851	18400	spectr.	4.41	1.7e-4 ±27%	–	–	3.5e-5	54±3.	80.
37017	1890	19200	spectr.	4.45	2.7e-5 ±28%	–	–	1.8e-5	∼80.±9.	170.
37479	1932	22200	spectr.	4.53	1.7e-5±22%	–	–	3.7e-5	∼100±15.	170.
37776	26742	21800	spectr.	4.52	6.0e-5 ±20%	–	–	3.2e-5	75±7.	160.
260858	S95920	19200	spectr.	4.22	6.0e-5 ±41%	–	–	1.5e-5	47±3.	<30.
264111	32581	23200	spectr.	4.54	9.0e-6 ±20%	–	–	3.0e-5	75±8.	140.
-27 3748	34781	22700	spectr.	4.53	1.4e-5±21%	–	–	7.0e-6	45±4.	160.
58260	35830	19000	spectr.	4.02	4.0e-5±38%	–	–	3.4e-5	45±6.	<30.
60344	36707	21700	spectr.	4.48	5.0e-5±21%	–	–	3.0e-5	55±6.	<30.
64740	3089	22700	spectr.	4.50	5.0e-5±20%	–	–	3.5e-5	130±9.	160.
66522	39246	18800	spectr.	4.39	3.7e-4 ±16%	3.1e-4 ±27%	2.0e-3 ±30%	8.2e-6	0. ±4.	<30.
-46 4639	LS 1169	22000	spectr.	4.52	8.7e-5 ±10%	1.1e-4±26%	5.7e-4±29%	3.7e-5	80. ±4.	150.
92938	4196	15000	spectr.	4.12	4.7e-4 ±29%	1.1e-4±31%	–	3.4e-5	125. ±4.	–
96446	54266	22000	spectr.	4.54	3.7e-5 ±11%	9.1e-5±22%	2.7e-5±29%	8.0e-6	0. ±4.	<30.
-62 2124	LS 2394	26000	spectr.	4.23	6.7e-5±21%	–	–	3.3e-5	75±8.	–
108483	4743	19100	spectr.	4.25	9.7e-5 ±37%	–	–	3.5e-5	130±12.	–
133518	73966	18600	spectr.	4.04	2.7e-4±17%	1.4e-4±32%	4.7e-4±33%	8.0e-6	0. ±4.	<30.
149257	N6178-1	24900	phot.	4.19	3.7e-5±9%	7.1e-5±19%	6.7e-5±27%	–	40. ±4.	70.
-69 2698	84185	25300	phot.	3.90	3.7e-5 ±9%	9.7e-5 ±19%	6.7e-5 ±28%	–	30. ±3.	50.
168785	S210064	23400	phot.	4.11	2.2e-5 ±10%	5.1e-5±24%	2.7e-4±29%	–	14. ±2.	70.
169467	6897	16600	phot.	4.05	2.7e-4 ±29%	2.1e-4±33%	6.7e-4±35%	–	30. ±3.	–
56139	2749	18000	phot.	3.63	4.7e-5±45%	–	–	3.6e-5	80.±7.	–
105435	4621	26000	phot.	4.51	8.7e-5±32%	–	–	–	∼240.±11.	–
121790	5249	19600	spectr.	4.42	9.7e-5±44%	–	–	3.2e-5	90.±8.	–
110879	4844	18200	spectr.	4.47	3.7e-4±27%	2.1e-4±20%	–	–	130. ±4.	–
122980	5285	19600	spectr.	4.44	2.7e-4±26%	2.8e-4±24%	6.7e-4±29%	3.7e-5	20. ±2.	–
144218	5985	20300	phot.	4.16	9.7e-5±17%	2.1e-4±24%	3.7e-4±30%	–	60. ±4.	–
solar		–	–	–	3.7e-4	1.1e-4	6.7e-4	3.4e-5	–	–
∑He-r		–	–	–	1.1e-4	1.3e-4	5.2e-4	2.6e-5	–	–
∑norm		–	–	–	1.6e-4	2.3e-4	5.2e-4	3.5e-5	–	–
Kilian		–	–	–	1.7e-4	5.3e-5	3.7e-4	2.7e-5	–	–

born (1983) based on low dispersion data, ~ 40 Åmm^{-1}, is also displayed. We can basically confirm Walborn's distribution, keeping in mind the small number of stars involved (we have 17 stars in common with Walborn), as well as the fact that most $v \sin i$ values of Walborn are larger than ours, as Table 1 shows. The spectral-type dependence of $vsini$ values show no significant trend. Fig. 5 shows that most He-rich stars have $v \sin i < 100$ km s^{-1}, with just a few around 130 km s^{-1}. Normal stars are more uniformly distributed, up to values as large as 350 km s^{-1}. The difference is probably significant, though the number of He-rich stars is small. This would indicate that slow rotation is characteristic of all main-sequence magnetic stars, including the He-rich ones. The K-S test has been applied to the cumulative distributions of normal and He-rich stars and has shown that the distributions differ from each other at a significance level of 98.5 percent, while the chi-square test applied to the binned distributions gave the same result, at a significance level of 98 percent.

6. Conclusions

Based on LTE model atmospheres and both low and high-resolution spectra, we present abundance analysis of a sample of 6 standard stars and 21 He-rich stars. Having used a standard synthetic spectrum method we achieved the following progress results:

- a lack of fast rotators
- given the atomic data a possible diverse pattern of abundances from under-solar up to over-solar values
- an underabundance of carbon in He-rich stars with respect to standard stars
- a solar abundance for the heavier element, magnesium

The results above suggest that observed CNO abundances do not entirely fulfil the predictions of the model proposed by Michaud et al. (1987), i.e. predicted solar values, and that this model should include not only the stellar wind but also the detailed magnetic geometry as well as the interaction

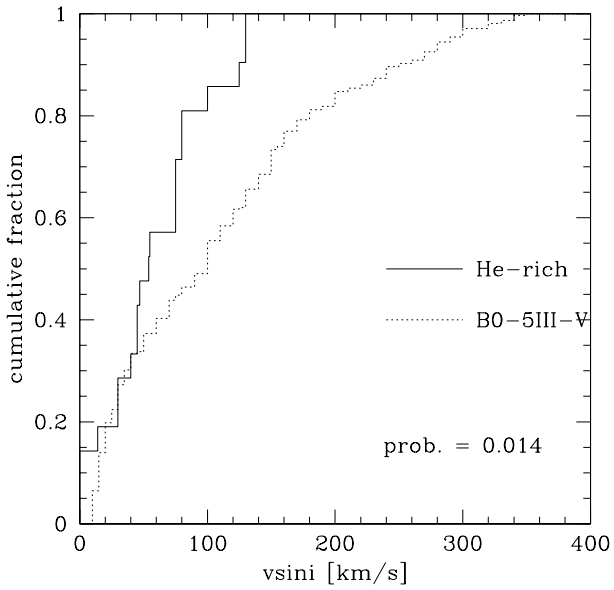

Fig. 6. The cumulative distributions of normal and He-rich stars.

of mass loss with it, as a next step to further progress. The agreement is reached however for the coolest He-rich stars, since they tend to have the same carbon abundance as standard stars, following the model predictions. The general carbon underabundance is also in agreement with the results of Hunger & Groote (1993) and paper V of Kilian (1994) as well as the nearly solar magnesium abundance. Another interesting result is that even normal stars like HD 122980 seem to have non-solar abundances (Fig. 1). The abundances are based on LTE model atmospheres and semi-empirical gf values from Kurucz & Peytremann (available e.g. in the CCP7 library) and may be less accurate than if they were based on full NLTE treatment, but they seem really different from one "standard" star to the other, even if their absolute value is less reliable. Kilian (1992) also found significant abundance variations among normal B stars which, however, are hotter on average than ours. The intercomparison of equivalent widths wherever possible with her paper is within 10–15%. She reached the statement that interstellar matter was well mixed on large scales, but inhomogeneous on small scales. Owing to the limited wavelength region of high-resolution data, the error bars and finally the LTE treatment, we cannot proceed to further considerations on the abundance spread. In particular, these limitations exceed another source of uncertainities such as semi-empirical atomic data. On the other hand, slow rotation of He-rich stars turned out to be a significant fact, in comparison with the rotational velocities of normal B type stars. Thus, slow rotation is characteristic of all magnetic main-sequence stars. We hope to obtain better abundance estimates in the near future, on the basis of new échelle spectra and of a more realistic interpretation, including NLTE treatment.

Acknowledgements. This research has made use of the Simbad database, operated at CDS, Strasbourg, France. PN thanks the Swiss National Science Foundation for its support. and the ESO staff for his help both in Garching and at La Silla.

References

Hunger K., Groote D., 1993, In: Dworetsky M.M., Castelli F.,Faraggiana R. (eds.) Peculiar versus Normal Phenomena in A-type and Related Stars. IAU Coll. No.138, ASP Conf. Series Vol.44, San Francisco, p. 394

Kilian J., 1992, A&A, 262, 171

Kilian J., 1994, A&A, 282, 867

Kurucz R.L., 1992, Rev. Mex. Astron. Astrofis. 23, 45

Michaud G., Dupuis J., Fontaine G., Montmerle T., 1987, ApJ 322, 302

Osmer P.S., Peterson D.M., 1974, ApJ 187, 117

Vauclair S., 1975, A&A 45, 233

Walborn N.R., 1983, ApJ 268, 195

Wolff S.C., Edwards S., Preston G.W., 1982 ApJ 252, 322

Zboril M., Glagolevskij Yu.V., North P., 1994, In: Zverko J., Žižňovský J. (eds.) International Conference on CP and Magnetic Stars. Tatranská Lomnica, p. 105

Zboril M., North P., Glagolevskij Yu.V., Betrix F., 1997, A&A 324, 949